DISCOVERY

To Cite:
Antwi BY, Cameron J, Findlay NJ, Owoare RB, Kingsford-Adaboh R, Skabara PJ. Synthesis of novel star-shaped truxene cored small molecules and applications in organic solar cells. *Discovery* 2023; 59: e113d1354
doi: https://doi.org/10.54905/disssi.v59i333.e113d1354

Author Affiliation:
[1]Department of Chemistry, University of Ghana, Legon, Accra, Ghana
[2]School of Chemistry, University of Glasgow, Glasgow, G12 8QQ, United Kingdom
[3]Council for Scientific and Industrial Research - Institute of Industrial Research, East-Legon, Accra, Ghana

[*]**Corresponding author**
Department of Chemistry, University of Ghana, School of Chemistry, University of Glasgow, Glasgow, G12 8QQ, United Kingdom, Council for Scientific and Industrial Research - Institute of Industrial Research, East-Legon, Accra, Ghana
Email: boniface.antwi@gmail.com

ORCID List

Boniface Y Antwi	0000-0002-7016-345X
Joseph Cameron	0000-0001-8622-8353
Neil J Findlay	0000-0001-6855-0998
Richard B Owoare	0000-0002-2270-0724
Robert Kingsford-Adaboh	0000-0002-2629-3783
Peter J Skabara	0000-0001-7319-0464

Peer-Review History
Received: 13 June 2023
Reviewed & Revised: 17/June/2023 to 26/September/2023
Accepted: 30 September 2023
Published: 04 October 2023

Peer-Review Model
External peer-review was done through double-blind method.

Discovery
pISSN 2278–5469; eISSN 2278–5450

DISCOVERY SCIENTIFIC SOCIETY

Synthesis of novel star-shaped truxene cored small molecules and applications in organic solar cells

Boniface Y Antwi[1,2,3*], **Joseph Cameron**[2], **Neil J Findlay**[2], **Richard B Owoare**[1], **Robert Kingsford-Adaboh**[1], **Peter J Skabara**[2]

ABSTRACT

The synthesis of two new star-shaped organic small molecules with a truxene core, molecules 11 and 12, were carried out. They varied in sidechain length with molecule 11 having hexahexyl and molecule 12 having hexadodecyl side chains. The physical and photovoltaic properties were measured and characterized. Both molecules showed activity in UV-visible light and electrochemical processes. Molecule 11 had optical and electrochemical HOMO-LUMO energy gaps of 2.15 and 2.45 eV, respectively, while molecule 12 had 2.12 and 2.50 eV gaps. Photovoltaic device fabrication and testing revealed bifunctional acceptor-donor properties of the molecules in bulk-heterojunction organic solar cells. The device PCEs for molecule 11 were 0.003% and 0.002%, while the PCEs for 12 were 0.004% and 0.03%. This improvement was attributed to the ease of processing and self-assembly induced by the long alkyl side chains of molecule 12.

Keywords: Synthesis; Star-shape; Truxene; Organic small molecules; Solar cells

1. INTRODUCTION

The unique two to three-dimensional geometry of star-shaped molecules make them attractive in varied optoelectronic applications such as colour converters Sajjad et al., (2017) organic light-emitting diodes (OLEDs) Chen et al., (2016), organic field effect transistors (OFET) Choi et al., (2014), perovskites Zhang et al., (2017), sensors Haughey et al., (2014), lasers Wang et al., (2013), organic solar cells (OSC) Ponomarenko et al., (2014), and so on (Jarosz et al., 2014). The linear π-conjugated arms for these molecules converge at a center generally described as the core. These arms and cores vary in molecular composition and electronic properties, which induce a multifunctional property of the star-shaped molecule (Belton et al., 2013; Kanibolotsky et al., 2004; Thomson et al., 2013).

The core, Figure 1, which was first synthesized by Kipping in 1894 Kipping, (1894) bears a heptacyclic polyarene structure with a *C3h* symmetry Kanibolotsky et al., (2010) that is functionalized at the periphery for diverse applications such as discotic liquid crystals Palmans and Meijer, (2007), non-linear optics (NLO) Po

et al., (2019), organogels Galisteo-López et al., (2015), OLEDs Yao et al., (2015), sensors Huang et al., (2017), OSC Zhang et al., (2016), fluorescent probes Earmrattana et al., (2012), dye-sensitized solar cells (DSSC) Wu et al., (2015), photoinitiators Xiao et al., (2015), perovskites Gao et al., (2017), organic lasers Haughey et al., (2014), and OFETs (Sun et al., 2005).

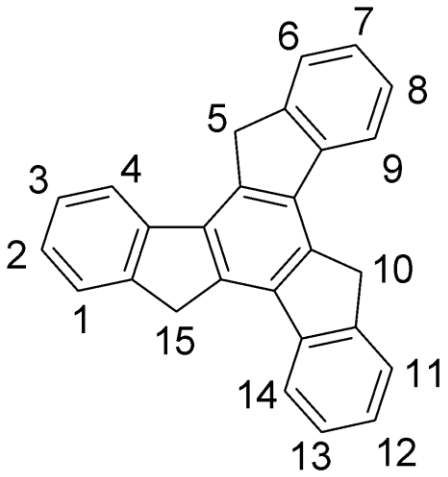

Figure 1 Structure of Truxene (Shi et al., 2015).

Functionalization of the truxene core is typically achieved at the C2, C7, and C12 positions, as well as the C5, C10, and C15 atoms. However, other positions can also be substituted. Alkyl groups are usually substituted at the C5, C10, and C15 positions (Shi et al., 2015). Furthermore, the incorporation of alkyl side chains is found to increase the solubility of the molecules, as well as, improve charge transport, morphology, and device performance (Gadisa et al., 2009). Additionally, these electronically inert alkyl side chains which are orthogonal to the truxene plane control packing through steric hindrance, even though they may hinder molecular π−π stacking (Roncali, 2007). The length and position of these side chains also contribute to the optoelectronic properties of the molecules (Huang et al., 2012; Tao et al., 2014).

Thiophene π-linkers have been utilized in the synthesis of scalable novel semiconducting organic molecules for solar cell applications (Bin et al., 2016). They induce stabilized planarity in the host molecule, through attractive heteroatom interactions (S-O/S-N), which may be fortified in crystal formation (Raychev and Guskova, 2017). This further improves the solid-state packing leading to favorable current density and charge transport properties (Schueppel et al., 2008). Additionally, the termination of novel semiconducting organic small molecules with the strong electron-withdrawing 3-ethyl rhodanine unit has been extensively utilized in organic solar cells (Antwi et al., 2016; Ni et al., 2015; Wan et al., 2017). This includes the synthesis of novel electron donors Fan et al., (2017) and non-fullerene acceptors (Holliday et al., 2015).

The electron-withdrawing thioketone and ketone groups on the rhodanine periphery increase the internal electronic push-pull (Privado et al., 2017). Therefore, end-capping scalable organic photoactive molecules with 3-ethyl rhodanine have been found to enhance the photovoltaic performance of molecules through an efficient HOMO-LUMO energy gap engineering, photon absorption, and favorable device morphology (Wu et al., 2018). Similarly, the 2D geometry and extended π−conjugations of truxene have been explored in the synthesis of non-fullerene acceptors Wu et al., (2018), electron donors Isla et al., (2012), and electron-collecting interlayers for organic solar cells (Xu et al., 2015). Here in, we report a newly synthesized truxene derivative achieved by coupling 3-ethyl rhodanine to the terminals of the truxene core through thiophene linkers. Substitution of hexahexyl and hexadodecyl chains at the C5, C10, and C15 positions were separately carried out to yield, molecules 11 and 12 respectively, (Scheme 1).

The physical properties as determined showed that the molecules were thermally stable with a 5% degradation temperature beyond 300 °C. Also, they exhibited sufficient photon absorption in visible light with a molar absorptivity constant between 1.63×105 (11) and 1.47×105 (12). Electrochemical processes displayed a HOMO-LUMO gap of 2.45 eV and 2.5 eV for 11 and 12 respectively. Organic solar cell applications showed a bifunctional property of the molecules. The molecules acted as both donor and acceptor units to PC61BM and P3TH respectively, even though their recorded photovoltaic performances were not as expected.

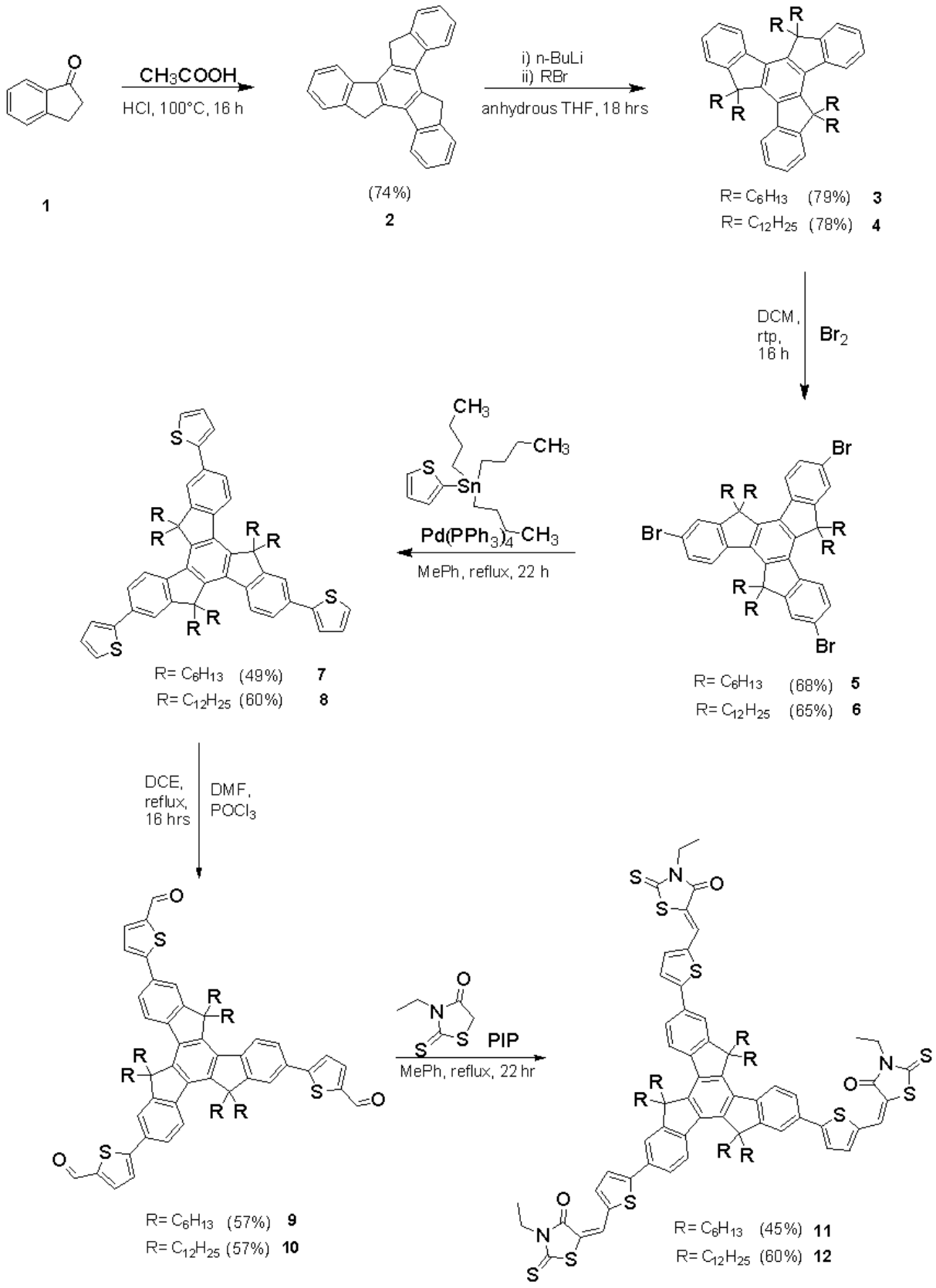

Scheme 1 Synthesis of target molecules 11 and 12.

2. METHODOLOGY

Truxene and reagents were purchased from Sigma-Aldrich at 99.9% purity. To a stirred suspension of truxene, (1 eq) in tetrahydrofuran (5.4 ml per gram) under nitrogen, n-BuLi (3.8 eq) was added dropwise at 0 °C over 30 min. The temperature was held below 15 °C for the duration of the addition. The truxene solid was dissolved and the colour changed to deep red, which disappeared during addition but persisted on the complete addition of n-BuLi. The solution was stirred at room temperature for 30 min then 1-bromoalkane (3.8 eq) was added over 10 min at 0 °C. The mixture was stirred at room temperature for 4 h and a second portion of n-BuLi (3.8 eq) was added over 10 min at 0 °C. After stirring at room temperature for 30 min, a second portion of 1-bromoalkane (3.8 eq) was added over 10 min at 0 °C. The reaction mixture was then stirred at room temperature for 18 h (TLC monitoring). Upon reaction completion, it was quenched with saturated aqueous ammonium chloride and extracted with petroleum ether (5 times).

The combined organic fractions were washed with water, dried over anhydrous MgSO4, and the solvent evaporated. The material was purified by column chromatography on silica gel, eluting with petroleum ether to yield the product. OPV device performances were investigated using the bulk-heterojunction architecture with indium tin oxide (ITO) and calcium as the electrodes and poly (3, 4-ethylene dioxythiophene): Polystyrene sulfonate (PEDOT: PSS) as a hole transport layer, with a device structure of glass/ITO/PEDOT: PSS/photoactive layer/Ca (40 nm)/Al (40 nm). The photoactive layer was processed from a chloroform solution of each small molecule donor and [6,6]- phenyl C_{71} butyric acid methyl ester ($PC_{71}BM$) acceptor, and small molecule acceptor with poly-3-hexylthiophene (P3HT) donor.

3. RESULTS AND DISCUSSION

The synthesis of the truxene core 2 was completed by the cyclotrimerization of 1-indanone 1 in an acidic medium, Scheme 1. The completed batch of truxene core was separated into two portions to allow alkylation using brominated hexyl and dodecyl alkanes. In this process, the three sp2 carbons of the truxene core were di-substituted to yield hexahexyltruxene 3 and hexadodecyltruxene 4 units, Scheme 1. The Truxene core had positions C2, C7, and C12 brominated as shown in compounds 5 and 6, Scheme 1, to facilitate the coupling of thienyl groups to the truxene core. Products 7 and 8 were only isolated following Stille cross-coupling reactions in moderate yields, Scheme 1. With compounds 7 and 8 in hand, subsequent formylation was attempted by lithiation, and Vilsmeier-Haak techniques to give compounds 9 and 10 moderate yields.

Formation of the targeted molecules was attempted via coupling the appropriate acceptor unit to molecules 9 and 10 using the Knoevenagel condensation reaction, Scheme 1. In the event, the 3-ethyl rhodanine acceptor was successfully coupled to both 9 and 10 to give compounds 11 and 12 as orange powders in 45% and 65% yield, respectively. Details of the above experiments, the NMR, DSC, MALDI-MS, and elementals are outlined in the supporting information, SI-1 to SI-5. The thermal stability of 11 and 12 was tested by thermogravimetric analysis. Thermograms of the molecules are shown in (Figure 2). The onsets of 5% degradation temperatures were found at 390.94 oC and 364.29 oC for 11 and 12, respectively, (Table 1). This is an indication that the molecules are suitably thermally stable for applications in organic solar cell fabrications.

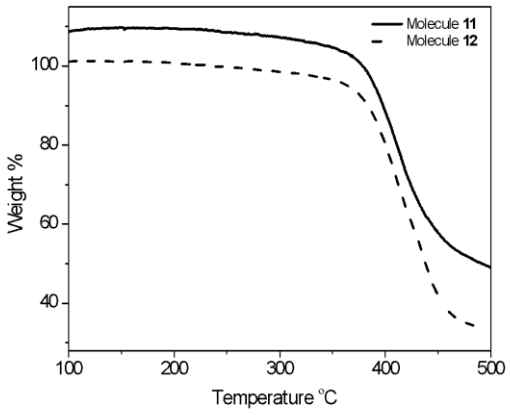

Figure 2 TGA plots of 11 and 12 measured at 10 °C min-1 under argon.

Table 1 Electrochemical, thermal, and optical characteristics of 11 and 12.

Compound	Optical measurements					Electrochemical measurements			Td (°C)
	Solution				Film				
	max (nm)	Egap (eV)	ε (L mol-1 cm-1)	max (nm)	Egap (eV)	HOMO (eV)	LUMO (eV)	Eg (eV)	
(11)	483	2.33	1.63×105	466	2.15	-5.37	-2.92	2.45	390.94
(12)	486	2.26	1.47×105	464	2.12	-5.73	-3.23	2.50	364.29

The optical properties of molecules 11 and 12 were determined by the UV-vis spectroscopic measurements. Plots of the normalized absorption spectra for the solution and solid state are shown in (Figure 3).

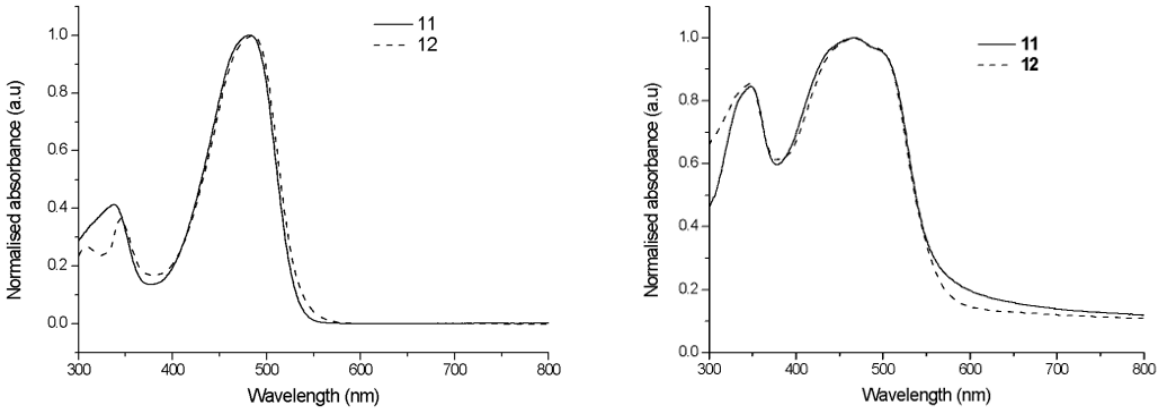

Figure 3 Normalized absorption spectra of 11, and 12 (a) in chloroform solution (10-5 M) and (b) drop cast film on quartz glass.

All molecules are absorbed in the UV-visible region with absorptions between 400 nm and 550 nm being the π-π*electronic transitions of the molecules in (Figure 3a, 3b) (Isla et al., 2012). In solution, 11 and 12 showed absorption maximums of 483 nm and 486 nm, respectively, (Figure 3a). Molecule 11 showed a slightly higher absorbance with an extinction coefficient of 1.63×105 L mol-1 cm-1, (Table 1). In the solid state, Figure 3b, a broader absorption peak compared to the narrow peak in solution indicates strong aggregation and packing of molecules when deposited as a film. The π-π stacking interaction of the molecules resulted in shoulder peaks in the solid state, for 11 at 499 nm and 12 at 497 nm compared to those in solution.

The difference in shoulder peaks can be attributed to the substituted alky chains on the molecules. It is anticipated that the strong aggregation of 11 due to hexahexyl chain substituents may have influenced the shoulder peak at 499 nm, while the octadecyl chain on 12 caused a weak aggregation, leading to a slightly lower shoulder peak at 497 nm. Both molecules 11 and 12 exhibited narrow optical HOMO-LUMO energy gaps, Table 1, which were calculated from the leading edge of absorptions. The HOMO-LUMO energy gap narrowed in the solid state for both molecules. 12 showed the narrower energy gap, 2.12 eV, compared to 2.15 eV for 11, in the solid state.

The oxidation and reduction potentials for 11 and 12 are shown in (Figure 4). They exhibited oxidation and reduction potentials in an electrochemical process, which indicates their ability to lose and gain electrons. 11 exhibited two oxidation potentials. One irreversible at +0.57 V and one reversible at half-wave potential +0.73 V. An irreversible reduction wave was observed at -1.87 V.

Similarly, 12 showed one irreversible oxidation and reduction process with potentials of +0.93 V and -1.57 V and one quasi-reversible oxidation wave with a half-wave potential of +1.10 V. The oxidation potentials are attributable to electrons lost by the thiophene linkers and the reduction waves due to the electron gained by 3-ethyl rhodanine acceptors (Xu et al., 2015). The molecules, 11 and 12**,** exhibited slightly different electrochemical HOMO-LUMO energy gaps, 2.45 eV and 2.50 eV respectively, which is backed by the dissimilar HOMOs (-5.37 vs 5.73 eV) and LUMOs (-2.92 vs -3.23), (Table 1). This is attributable to the different lengths of the alkyl sidechains on 11 and 12.

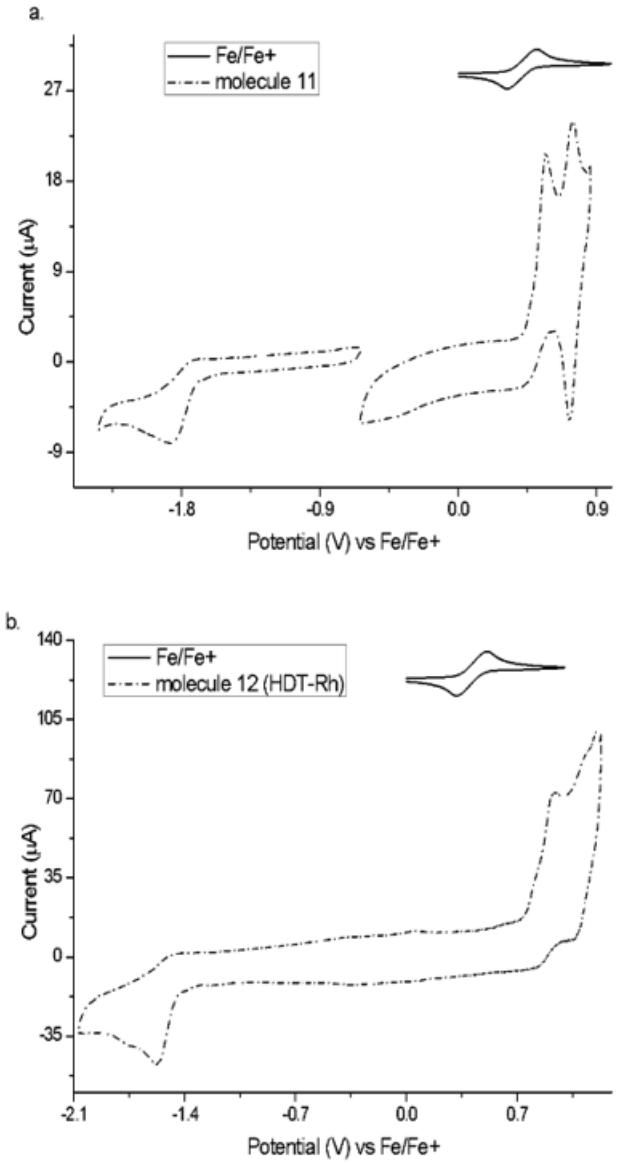

Figure 4 Cyclic voltammograms of 11 (a), and 12 (b) in dichloromethane solution (10-4 M) with Bu4NPF6 as the supporting electrolyte (0.1 M), recorded at a scan rate of 100 mV s-1.

Furthermore, the photovoltaic performances of target molecules 11 and 12 were investigated. These molecules acted separately as electron donors (D) to the fullerene derivative PC61BM acceptor (A) and as electron acceptors to P3HT donor (D) in binary bulk-heterojunction organic solar cells. Devices for P3HT: PC61BM blend acted as references since they have been extensively studied in organic solar cells (Dang et al., 2011). They were optimized at a 1:1 D/A ratio and an annealing temperature of 140°C. Fabricated devices of 11 and 12 were optimized at the same annealing temperature as P3HT: PC61BM reference. However, the D/A ratios were varied (1:1, 1:2, 1:3, and 1:4). The devices were then tested and data recorded, Table 2, and Figure 5 (a-e).

Table 2 Table of best device performances for 11 and 12

Device composition	Jsc (mA cm – 2)	Voc (V)	FF	PCE (%)
11_PC61BMc	0.03	0.40	0.26	0.003 ± 14E-4
12_PC61BMd	0.04	0.34	0.28	0.004 ± 2E-3
P3HT_PC61BMa	4.49	0.48	0.52	1.140 ± 3E-1
P3HT_11b	0.02	0.34	0.23	0.002 ± 1E-3
P3HT_12 b	0.24	0.76	0.16	0.030 ± 4E-3

D/A ratios; a1:1, b1:2, c1:3 and d1:4.

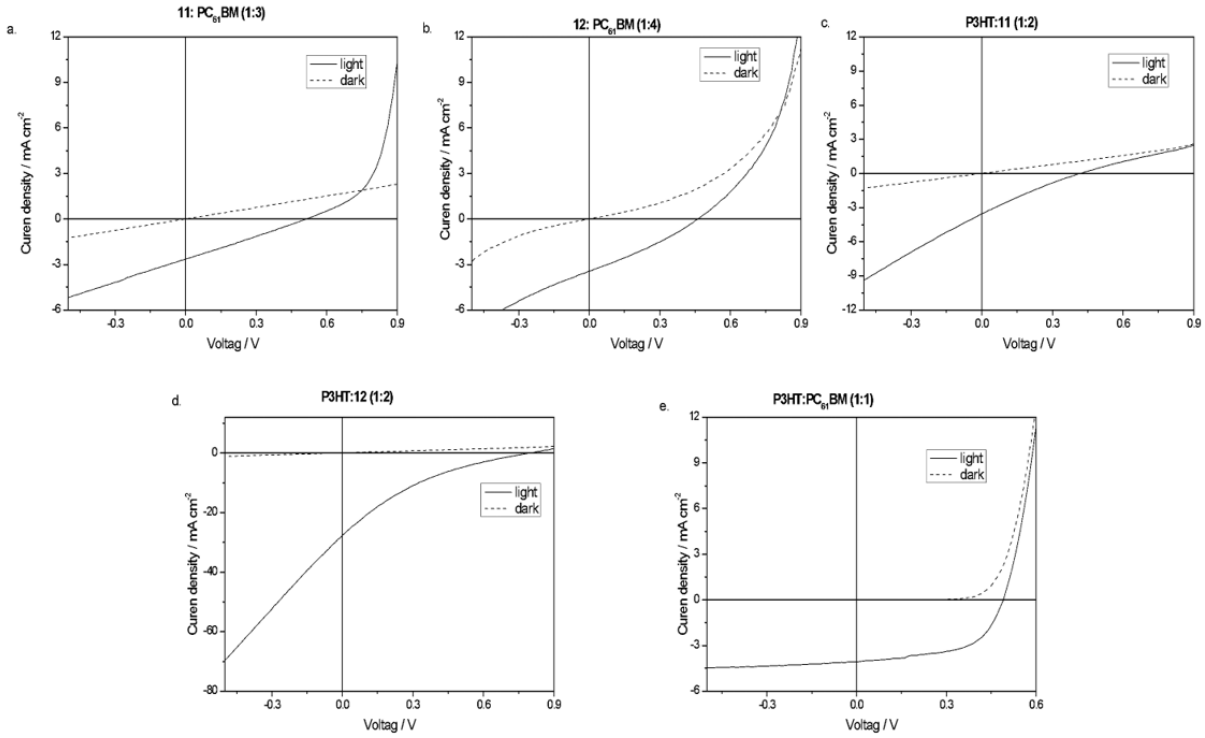

Figure 5 Current-Voltage plot of best performing devices for a. 11_PC61BM, b. 12_PC61BM, c. P3HT_11, d. P3HT_12 and e. P3HT: PC61BM reference device.

The devices for molecules 11 and 12 showed photovoltaic performances either as donor or acceptor units in bulk-heterojunction organic solar cells. However, their power conversion efficiencies (PCE) were less impressive, which fell below that of the reference device (P3HT_PC61BM), Table 2, and Figure 5 (a-e). Nonetheless, as separate donors to PC61BM acceptor, 12 exhibited a better device performance over 11, (Table 2). At 1:4 D/A ratio 12 displayed a PCE (0.004±2E-3), Voc (0.34 V), FF (0.28), and Jsc (0.04 mA cm-2). Whilst 11 showed a PCE (0.003±14E-4), with Voc (0.40 V), FF (0.26), and Jsc (0.03 mA cm-2), at a D/A ratio of 1:3. The slightly better performance of 12 over 11 is attributable to the more solubilizing dodecyl chains which may have improved the morphology of fabricated devices leading to Jsc (0.04 vs 0.03 mA cm-2) and PCE (0.004±2E-3 vs 0.003±14E-4), (Figure 5a, 5b).

Likewise, as electron acceptors to P3HT, 12 demonstrated better device performance over 11. It exhibited a PCE (0.03±4E-3%) with Voc (0.76 V), FF (0.17), and Jsc (0.24 mA cm-2) against that of 11 PCE (0.002±1E-3%), Voc (0.34 V), FF (0.23) and Jsc (0.02 mA cm-2), all at a D/A ratio of 1:2. This is attributable to the better Voc (0.76 vs 0.34 V) and Jsc (0.24 vs 0.02 mA cm-2) of 12 against 11, (Figure 5c, 5d). The superior Jsc (0.24 mA cm-2) of 12 over 11 Jsc (0.02 mA cm-2) is attributable to the close match of the LUMO and HOMO energy levels for 12 and P3HT (3.2 vs 3.2 eV and 5.7 vs 5.1 eV), compared to that of 11 and P3HT (2.9 vs 3.2 eV and 5.4 vs 5.1 eV).[52] The LUMO (3.2 vs 3.2) and HOMO (5.7 vs 5.1) energy levels for 12 and P3HT promoted electron extraction and hole transport to the electrodes at a power conversion efficiency of 0.03%, which is an over tenfold efficiency compared to 0.002% for 11. Additionally, the favorable device morphology induced by the pendant dodecyl chains and the complimentary absorption of 12 in the visible region contributed to its better performance over 11.

4. CONCLUSION

Two truxene derivatives 11 and 12 bearing hexahexyl and hexadodecy pendant chains on the backbone have been successfully synthesized. Their physical and photovoltaic properties have been measured and characterized. The optical and electrochemical HOMO-LUMO energy gaps were 2.15 and 2.45 eV for 11 and, 2.12 and 2.50 eV for 12 respectively. They showed photovoltaic performances as electron-donating and withdrawing units in a binary bulk-heterojunction solar cell and indicated their potential to act as bifunctional molecules which could be explored in ternary bulk-heterojunction organic solar cells. Molecule 12**,** displayed a better device performance (PCE of 0.03%), as an electron acceptor, compared to 11 (PCE of 0.002%).

Therefore, the better optoelectronic performance of 12 over 11 confirms that long alkyl side chains of organic semiconductors contribute to improving the HOMO-LUMO energy gaps and the photovoltaic performances (Fu et al., 2017). During the course of preparing this manuscript, we became aware of the publication of molecule 11 used only as a small molecule non-fullerene acceptor

in solar cells (Lin et al., 2022). Herein, the bifunctional properties of compounds 11 and 12 in organic solar cell applications is reported for the first time.

Author Contributions

Boniface Antwi and Joseph Cameron drafted the manuscript. The manuscript was reviewed by Neil Findlay, Richard Owoare, Robert Kingsford-Adaboh, and Peter Skabara.

Informed consent

Not applicable.

Ethical approval

Not applicable.

Conflicts of interests

The authors declare that there are no conflicts of interest.

Funding

This work received funding from the Royal Society - Leverhulme Africa Award (A4130029).

Data and materials availability

All data associated with this study are present in the paper.

REFERENCES AND NOTES

1. Antwi BY, Taylor RGD, Cameron J, Owoare RB, Kingsford-Adaboh R, Skabara PJ. Acceptor–donor–acceptor small molecules based on derivatives of 3,4-ethylenedioxythiophene for solution processed organic solar cells. RSC Adv 2016; 6 (101):98797-98803. doi: 10.1039/C6RA22897F
2. Belton CR, Kanibolotsky AL, Kirkpatrick J, Orofino C, Elmasly SET, Stavrinou PN, Skabara PJ, Bradley DDC. Location, Location, Location - Strategic Positioning of 2,1,3-Benzothiadiazole Units within Trigonal Quaterfluorene-Truxene Star-Shaped Structures. Adv Funct Mater 2013; 23 (22):2792-2804. doi: 10.1002/adfm.2_01202644
3. Bin H, Zhang ZG, Gao L, Chen S, Zhong L, Xue L, Yang C, Li Y. Non-Fullerene Polymer Solar Cells Based on Alkylthio and Fluorine Substituted 2D-Conjugated Polymers Reach 9.5% Efficiency. J Am Chem Soc 2016; 138(13):4657-4664. doi: 10.1021/jacs.6b01744
4. Chen L, Zhang C, Lin G, Nie H, Luo W, Zhuang Z, Ding S, Hu R, Su S-J, Huang F, Qin A, Zhao Z, Tang BZ. Solution-processable, star-shaped bipolar tetraphenylethene derivatives for the fabrication of efficient nondoped OLEDs. J Mater Chem C 2016; 4(14):2775-2783. doi: 10.1039/C5TC02949J
5. Choi H, Paek S, Lim N, Lee YH, Nazeeruddin MK, Ko J. Efficient perovskite solar cells with 13.63 % efficiency based on planar triphenylamine hole conductors. Chemistry 2014; 20 (35):10894-10899. doi: 10.1002/chem.201403807
6. Dang MT, Hirsch L, Wantz G. P3HT:PCBM, Best Seller in Polymer Photovoltaic Research. Adv Mater 2011; 23(31):3597-3602. doi: 10.1002/adma.201100792
7. Earmrattana N, Sukwattanasinitt M, Rashatasakhon P. Water-soluble anionic fluorophores from truxene. Dyes Pigm 2012; 9 3(1–3):1428-1433. doi: 10.1016/j.dyepig.2011.10.009
8. Fan M, Duan L, Zhou Y, Wen S, Li F, Liu D, Sun M, Yang R. Rhodanine side-chained thiophene and indacenodithiophene copolymer for solar cell applications. Mater Today Energy 2017; 5:287-292. doi: 10.1016/j.mtener.2017.07.007
9. Fu H, Meng D, Meng X, Sun X, Huo L, Fan Y, Li Y, Ma W, Sun Y, Wang Z. Influence of alkyl chains on photovoltaic properties of 3D rylene propeller electron acceptors. J Mater Chem A 2017; 5(7):3475-3482. doi: 10.1039/C6TA09049D
10. Gadisa A, Oosterbaan WD, Vandewal K, Bolsée J-C, Bertho S, D'Haen J, Lutsen L, Vanderzande D, Manca JV. Effect of Alkyl Side-Chain Length on Photovoltaic Properties of Poly(3-alkylthiophene)/PCBM Bulk Heterojunctions. Adv Func Mat 2009; 19(20):3300-3306. doi: 10.1002/ADFM.200900797
11. Galisteo-López JF, Gómez-Esteban S, Gómez-Lor B, López C. Tunable emission in dye-doped truxene-based organogels through RET. J Mater Chem C 2015; 3(22):5764-5768. doi: 10.1039/C5TC00706B
12. Gao Y, Hong Y-L, Yin L-C, Wu Z, Yang Z, Chen M-L, Liu Z, Ma T, Sun D-M, Ni Z, Ma X-L, Cheng H-M, Ren W. Ultrafast

Growth of High-Quality Monolayer WSe2 on Au. Adv Mater 2017; 29:1700990. doi: 10.1002/adma.201700990

13. Haughey A-M, Foucher C, Guilhabert B, Kanibolotsky AL, Skabara PJ, Burley G, Dawson MD, Laurand N. Hybrid organic semiconductor lasers for bio-molecular sensing. Faraday Discuss 2014; 174(0):369-381. doi: 10.1039/C4FD00091A
14. Holliday S, Ashraf RS, Nielsen CB, Kirkus M, Röhr JA, Tan C-H, Collado-Fregoso E, Knall A-C, Durrant JR, Nelson J, McCulloch I. A Rhodanine Flanked Nonfullerene Acceptor for Solution-Processed Organic Photovoltaics. J Am Chem Soc 2015; 137(2):898-904. doi: 10.1021/ja5110602
15. Huang W, Smarsly E, Han J, Bender M, Seehafer K, Wacker IU, Schröder RR, Bunz UHF. Truxene-Based Hyperbranched Conjugated Polymers: Fluorescent Micelles Detect Explosives in Water. ACS Appl Mater Interfaces 2017; 9(3):3068-3074. doi: 10.1021/acsami.6b12419
16. Huang Y, Zhang M, Ye L, Guo X, Han CC, Li Y, Hou J. Molecular energy level modulation by changing the position of electron-donating side groups. J Mater Chem 2012; 22(12):5700-5705. doi: 10.1039/C2JM16474D
17. Isla H, Grimm B, Pérez EM, Rosario-Torres M, Ángeles-Herranz M, Viruela R, Aragó J, Ortí EM. Guldi D, Martín N. Bowl-shape electron donors with absorptions in the visible range of the solar spectrum and their supramolecular assemblies with C60. Chem Sci 2012; 3(2):498-508. doi: 10.1039/C1SC00669J
18. Jarosz T, Lapkowski M, Ledwon P. Advances in star-shaped π-conjugated systems: properties and applications. Macromol Rapid Commun 2014; 35(11):1006-1032. doi: 10.1002/marc.201400061
19. Kanibolotsky AL, Berridge R, Skabara PJ, Perepichka IF, Bradley DDC, Koeberg M. Synthesis and Properties of Monodisperse Oligofluorene-Functionalized Truxenes: Highly Fluorescent Star-Shaped Architectures. J Am Chem Soc 2004; 126(42):13695-13702. doi: 10.1021/ja039228n
20. Kanibolotsky AL, Perepichka IF, Skabara PJ. Star-shaped π-conjugated oligomers and their applications in organic electronics and photonics. Chem Soc Rev 2010; 39(7):2695-2728. doi: 10.1039/B918154G
21. Kipping FS. XXIX. The formation of the hydrocarbon "truxene" from phenylpropionic acid, and from hydrindone. J Chem Soc Trans 1894; 65(0):269-290. doi: 10.1039 /CT8946500269
22. Lin K, Du W, Shen S, Liang H, Zhang X, Xiao M, Wang Y. Truxene-Centered Electron Acceptors for Non-Fullerene Solar Cells: Alkyl Chain and Branched Arm Engineering. Int J Mol Sci 2022; 23(18). doi: 10.3390/ijms231810402
23. Ni W, Li M, Wan X, Zuo Y, Kan B, Feng H, Zhang Q, Chen Y. A new oligobenzodithiophene end-capped with 3-ethyl-rhodanine groups for organic solar cells with high open-circuit voltage. Sci China Chem 2015; 58(2):339-346. doi: 10.1007/s11426-014-5220-x
24. Palmans ARA, Meijer EW. Amplification of Chirality in Dynamic Supramolecular Aggregates. Angew Chem Int Ed 2007; 46(47):8948-8968. doi: 10.1002/anie.200701285
25. Po C, Tao C-H, Li K-F, Chan CKM, Fu HL-K, Cheah K-W, Yam VW-W. Design, luminescence and non-linear optical properties of truxene-containing alkynylplatinum(II) terpyridine complexes. Inorganica Chim Acta 2019; 488:214-218. doi: 10.1016/j.ica.2018.12.030
26. Ponomarenko SA, Luponosov Yn, Fau-Min J, Min J, Fau-Solodukhin AN, Solodukhin An, Fau-Surin NM, Surin Nm, Fau-Shcherbina MA, Shcherbina Ma, Fau-Chvalun SN, Chvalun Sn, Fau-Ameri T, Ameri T, Fau-Brabec C, Brabec C. Design of donor-acceptor star-shaped oligomers for efficient solution-processible organic photovoltaics. Faraday Discuss 2014; 174:313-339. doi: 10.1039/c4fd00142g
27. Privado M, Cuesta V, de la Cruz P, Keshtov ML, Singhal R, Sharmad GD, Langa F. Efficient Polymer Solar Cells with High Open-Circuit Voltage Containing Diketopyrrolopyrrole-Based Non-Fullerene Acceptor Core End-Capped with Rhodanine Units. ACS Appl Mater Interfaces 2017; 9(13):11739-11748. doi: 10.1021/acsami.6b15717
28. Raychev D, Guskova O. (Charge carrier mobility in one-dimensional aligned π-stacks of conjugated small molecules with a benzothiadiazole central unit. Phys Chem Chem Phys 2017; 19(12):8330-8339. doi: 10.1039/C7CP00798A
29. Roncali J. Molecular Engineering of the Band Gap of π-Conjugated Systems: Facing Technological Applications. Macromol Rapid Commun 2007; 28(17):1761-1775. doi: 10.1002/marc.200700345
30. Sajjad MT, Manousiadis PP, Orofino C, Kanibolotsky AL, Findlay NJ, Rajbhandari S, Vithanage DA, Chun H, Faulkner G, O'Brien DC, Skabara PJ, Turnbull GA, Samuel I. A saturated red color converter for visible light communication using a blend of star-shaped organic semiconductors. Appl Phys Lett 2017; 110:013302. doi: 10.1063/1.4971823
31. Schueppel R, Schmidt K, Uhrich C, Schulze K, Wynands D, Brédas JL, Brier E, Reinold E, Bu HB, Baeuerle P, Maennig B, Pfeiffer M, Leo K. Optimizing organic photovoltaics using tailored heterojunctions: A photoinduced absorption study of oligothiophenes with low band gaps. Phys Rev B 2008; 77(8):085311. doi: 10.1103/PhysRevB.77.085311
32. Shi K, Wang Jy, Fau-Pei J, Pei J. π-Conjugated aromatics based on truxene: synthesis, self-assembly, and applications. Chem Rec 2015; 15(1):52-72. doi: 10.1002/tcr.201402071
33. Sun YM, Xiao K, Liu YQ, Wang JL, Pei J, Yu G, Zhu DB. Oligothiophene-Functionalized Truxene: Star-Shaped

Compounds for Organic Field-Effect Transistors. Adv Funct Mater 2005; 15(5):818-822. doi: 10.1002/adfm.200400380

34. Tao R, Umeyama T, Kurotobi K, Imahori H. Effects of Alkyl Chain Length and Substituent Pattern of Fullerene Bis-Adducts on Film Structures and Photovoltaic Properties of Bulk Heterojunction Solar Cells. ACS Appl Mater Interfaces 2014; 6(19):17313-17322. doi: 10.1021/am5058794
35. Thomson N, Kanibolotsky AL, Cameron J, Tuttle T, Findlay NJ, Skabara PJ. Incorporation of perfluorohexyl-functionalised thiophenes into oligofluorene-truxenes: synthesis and physical properties. Beilstein J Org Chem 2013; 9:1243–1251. doi: 10.3762/bjoc.9.141
36. Wan Z, Jia C, Wang Y, Yao X. A Strategy To Boost the Efficiency of Rhodanine Electron Acceptor for Organic Dye: From Nonconjugation to Conjugation. ACS Appl Mater Interfaces 2017; 9(30):25225-25231. doi: 10.1021/acsami.7b04233
37. Wang Y, Morawska PO, Kanibolotsky AL, Skabara PJ, Turnbull GA, Samuel IDW. LED pumped polymer laser sensor for explosives. Laser Photonics Rev 2013; 7(6):L71-L76. doi: 10.1002/lpor.201300072
38. Wu F, Liu J-L, Lee LTL, Chen T, Wang M, Zhu L-N. Dye-sensitized solar cells based on functionalized truxene structure. Chin Chem Lett 2015; 26(8):955-962. doi: 10.1016/j.cclet.2015.03.008
39. Wu W, Zhang G, Xu X, Wang S, Li Y, Peng Q. Wide Bandgap Molecular Acceptors with a Truxene Core for Efficient Nonfullerene Polymer Solar Cells: Linkage Position on Molecular Configuration and Photovoltaic Properties. Adv Funct Mater 2018; 28(18):1707493. doi: 10.1002/adfm.201707493
40. Xiao P, Zhang J, Dumur F, Tehfe MA, Morlet-Savary F, Graff B, Gigmes D, Fouassier JP, Lalevée J. Visible light sensitive photoinitiating systems: Recent progress in cationic and radical photopolymerization reactions under soft conditions. Prog Polym Sci 2015; 41:32-66. doi: 10.1016/j.progpolymsci.2014.09.001
41. Xu W, Kan Z, Ye T, Zhao L, Lai W-Y, Xia R, Lanzani G, Keivanidis PE, Huang W. Correction to Well-Defined Star-Shaped Conjugated Macroelectrolytes as Efficient Electron-Collecting Interlayer for Inverted Polymer Solar Cells. ACS Appl Mater Interfaces 2015; 7(8):5038-5038. doi: 10.1021/am506470b
42. Yao C, Yu Y, Yang X, Zhang H, Huang Z, Xu X, Zhou G, Yue L, Wu Z. Effective blocking of the molecular aggregation of novel truxene-based emitters with spirobifluorene and electron-donating moieties for furnishing highly efficient non-doped blue-emitting OLEDs. J Mater Chem C 2015; 3(22):5783-5794. doi: 10.1039/C5TC01018G
43. Zhang F, Wang Z, Zhu H, Pellet N, Luo J, Yi C, Liu X, Liu H, Wang S, Li X, Xiao Y, Zakeeruddin SM, Bi D, Grätzel M. Over 20% PCE perovskite solar cells with superior stability achieved by novel and low-cost hole-transporting materials. Nano Energy 2017; 41:469-475. doi: 10.1016/j.nanoen.2017.09.035
44. Zhang G, Lan Z-A, Wang X. Conjugated Polymers: Catalysts for Photocatalytic Hydrogen Evolution. Angew Chem Int Ed 2016; 55(51):15712-15727. doi: 10.1002/anie.201607375